Journal of Bioenergetics and Biomembranes, Vol. 35, No. 6, December 2003 (© 2003)

Calcium Channels: Unanswered Questions

Stephen W. Jones[1]

Despite decades of intensive research, many questions remain unresolved regarding the structure and function of voltage-dependent calcium channels. This review considers some of those questions: Where is the activation gate? Where are the inactivation gates? How are the voltage sensors coupled to the gates? Are bacterial K^+ channels good models for the Ca^{2+} channel pore? Are protein–protein interactions fundamental to Ca^{2+} channel function? Do voltage-dependent Ca^{2+} channels regulate basal intracellular Ca^{2+}? Are N and P/Q channels specialized for fast neurotransmitter release?

KEY WORDS: Gating; permeation; activation; inactivation; modulation; subunit; transmitter release; voltage; allosteric model.

When Dr. Maureen McEnery invited me to contribute an introduction to this collection of Ca^{2+} channel reviews, I realized that I did not want to simply update the overview from 5 years ago (Jones, 1998). As the other reviews in this issue will surely indicate, this does not reflect a lack of progress in the field. Yet an uncomfortably large number of "big" questions about Ca^{2+} channels remain unanswered, including a few that we (as a field) do not even seem to be trying to address effectively. Of course, the standard excuse is technical limitations. Quite correctly, we are all trained to choose projects where questions can be approached using existing techniques. If those techniques are new, even the better, as fads and fashions are not unknown to Science (and Nature, Cell, etc.). However, we may occasionally need to be reminded of the ultimate goals of our research. This review will examine questions central to our understanding of Ca^{2+} channels: how do they work, and what are they good for? Please see other reviews in this issue for other key questions, notably the role of normal and mutant Ca^{2+} channels in disease (Flink and Atchison, in press).

GATING

Mammalian genomes contain 10 genes coding for the primary ($\alpha 1$) subunits of voltage-dependent Ca^{2+} channels (Fig. 1). Both structurally and functionally, the primary division is between high voltage-activated (HVA) channels, crucial for muscle contraction and neurotransmitter release, vs. low voltage-activated (LVA) channels, involved in generation of repetitive electrical activity. There are two subfamilies among HVA channels, dihydropyridine-sensitive L-channels (Ca_v1) and others (Ca_v2). Typical invertebrate genomes contain one channel from each subfamily (Ca_v1, Ca_v2, and Ca_v3).

Ca^{2+} channels are members of the superfamily of voltage-dependent cation channels (Hille, 2001). This superfamily is characterized by a module containing six predicted transmembrane segments (S1–S6), plus a pore loop (P) that dips partially into the membrane. A single channel contains four such domains, either from four separate subunits (e.g., K^+ channels), or linked together in a single polypeptide chain (Ca^{2+} and Na^+ channels) (Fig. 2(A)). Each domain contains one unusual transmembrane segment that contains several positively charged amino acids. The molecular mechanism of voltage sensing is believed to be movement of these S4 segments through the transmembrane electrical field. This implies that a voltage-dependent channel is an allosteric protein: a single pore (formed by the four P loops) is regulated by four separate voltage sensors (Fig. 2(B)). The fundamental question is how voltage sensor movement is coupled to opening and closing of the ion-selective pore.

Studies of the molecular mechanisms of voltage-dependent gating are most advanced for K^+ channels, followed by Na^+ channels, with Ca^{2+} channels a poor third. K^+ channels are simpler than Na^+ and Ca^{2+} channels, as

[1] Department of Physiology and Biophysics, Case Western Reserve University, Cleveland, Ohio 44106; e-mail: swj@cwru.edu.

0145-479X/03/1200-0461/0

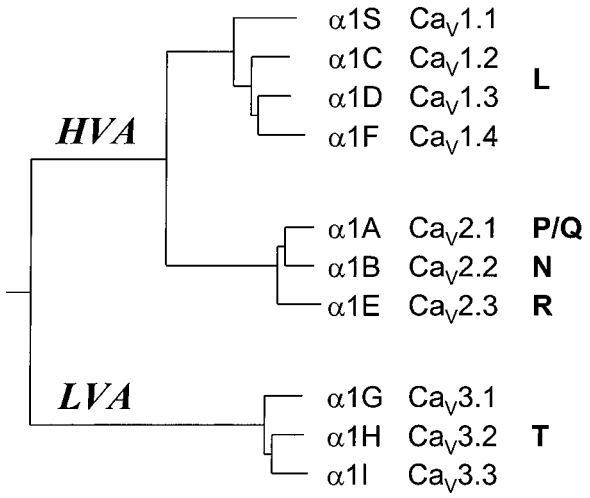

Fig. 1. A family tree for mammalian Ca^{2+} channels. Human $\alpha 1$ sequences were manually aligned, and conserved regions (excluding the N- and C-termini, and the I–II and II–III intracellular loops) were analyzed by the Phylip phylogeny package v. 3.5c, using the ProtDist and Fitch programs. Additional analysis (not shown) indicates that the LVA–HVA split is very close to the point of divergence of Na^+ from Ca^{2+} channels. Four classification schemes are shown: high vs. low voltage-activated (HVA vs. LVA); the single-letter notation for the $\alpha 1$ subunits ($\alpha 1$S for the Ca^{2+} channel of skeletal muscle, and $\alpha 1$B–$\alpha 1$I alphabetically); the new standard Ca_V classification (Ertel *et al.*, 2000); and the physiological classification based on kinetic and pharmacological properties (P/Q, N, R, L, and T). At one time, P and Q channels were proposed to be distinct entities, but they now appear to be extremes of a continuum, resulting at least in part from alternative splicing of a single gene (Bourinet *et al.*, 1999).

they can form homooligomers with four-fold symmetry. A single point mutation is automatically replicated four times in each channel. Furthermore, high resolution X-ray crystal structures are now known for several bacterial K^+ channels, including one member of the voltage-dependent cation channel superfamily (Jiang *et al.*, 2003a).

The K^+ channel structures have been remarkably informative mechanistically. Surprisingly, the S4 domain is on the outside of the molecule, and is essentially cytoplasmic in the crystal of the channel in its closed state. Apparently the S4 (together with part of S3) forms a "voltage-sensor paddle" that moves a large distance through the membrane in response to depolarization (Jiang *et al.*, 2003b).

One theme of this review will be speculation on whether the K^+ channel structures are likely to be good models for understanding Ca^{2+} channel function as well. Regarding gating, the conservation of the voltage-sensing module (together with more limited conservation of the pore module) encourages the view that the fundamental mechanism of voltage-dependent gating has been conserved among K^+, Na^+, and Ca^{2+} channels, from bacteria to humans.

Where Is the Activation Gate?

Classically, voltage-dependent channels are either fully open or fully closed at any given time. This means that a channel gates in a concerted manner, converting among distinct conformations where the ionic conductance of the channel is either maximal, or zero. In reality, "subconductance" states are occasionally observed, and may be informative about gating mechanisms (Chapman *et al.*, 1997; Zheng and Sigworth, 1998), but this will not be considered further here.

What is gating? The simplest picture is that a "gate" is literally a gate, a piece of the protein that physically occludes the pore when the channel is closed, and moves out of the way when the channel is open. That is believed to occur for N-type inactivation of K^+ channels (Hoshi *et al.*, 1990), but more subtle mechanisms are equally possible. Any conformational change in the channel protein that prevents ion flow would produce gating. This is usually pictured as a steric effect (a narrowing of the pore that ions cannot pass by), but any interference with the energy profile experienced by a permeating ion could effectively prevent ion movement (either high "barriers" or deep "wells").

For K^+ channels, electrophysiological (Armstrong, 1971; Del Camino *et al.*, 2000) and crystallographic (Jiang *et al.*, 2002) evidence points to an activation gate near the cytoplasmic end of the S6 helix.

Hints about the location of the Ca^{2+} channel gate come from the kinetics of block by Cd^{2+}. Cd^{2+} is thought to block the pore by binding tightly to the Ca^{2+} selectivity filter, thus preventing ion flux. For N-type Ca^{2+} channels, Cd^{2+} block of the open channel is voltage-dependent, such that strong hyperpolarization drives Cd^{2+} through the channel into the cytoplasm (Swandulla and Armstrong, 1989), while strong depolarization drives Cd^{2+} out into the extracellular space (Thévenod and Jones, 1992). However, the resting closed channel is blocked by Cd^{2+} with high affinity, even at strongly hyperpolarized voltages. That implies that Cd^{2+} cannot (easily) exit a closed channel to the intracellular space, as expected if there is a gate on the intracellular side of the pore. However, when extracellular Cd^{2+} is rapidly applied to closed channels, Cd^{2+} block develops ~100-fold more slowly than when the channels are open. Furthermore, relief of Cd^{2+} block is also ~100-fold slower if the channels are closed when Cd^{2+} is rapidly washed out. Taken literally, these results imply that a closed Ca^{2+} channel is closed at both ends of the pore

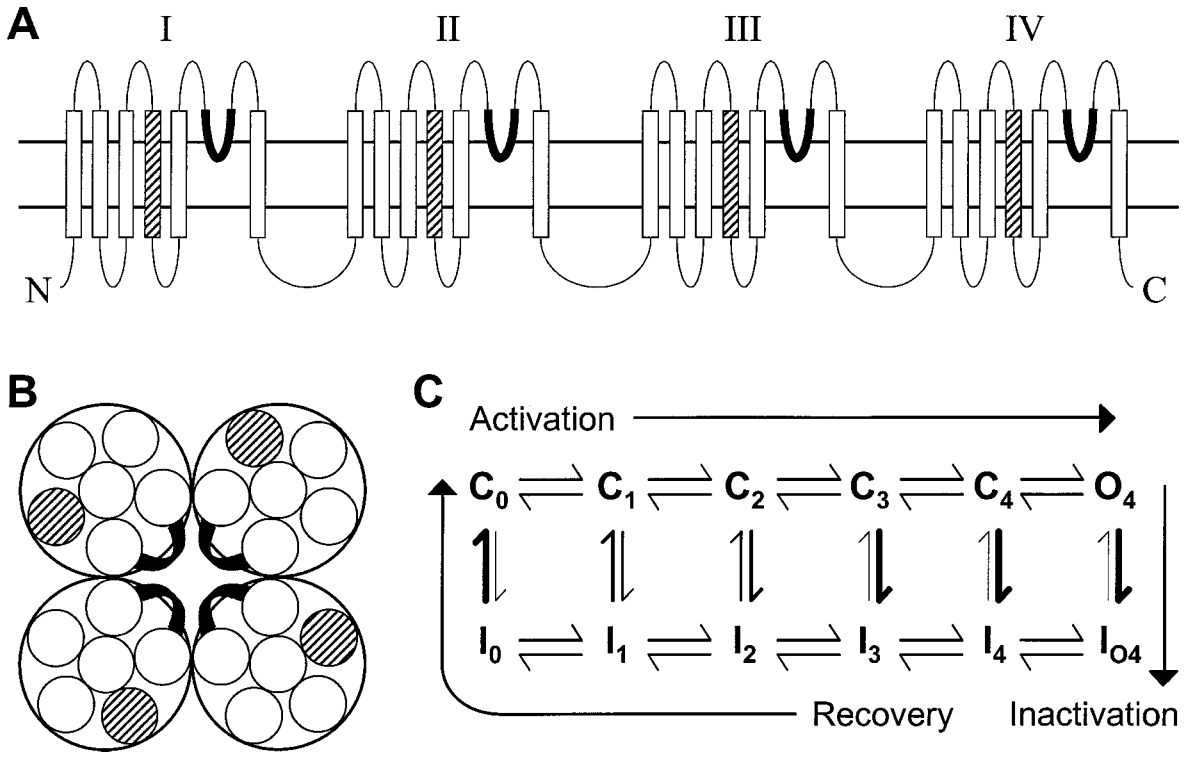

Fig. 2. Domain architecture of Ca^{2+} channels. (A) The hypothetical transmembrane architecture of a Ca^{2+} channel $\alpha 1$ subunit. The P loops are shown by solid curves, the S4 transmembrane segments as diagonally hatched bars, and other transmembrane segments as open bars. Note the four internally repeated units, labelled I–IV. The length of the intracellular and extracellular loops are variable among Ca^{2+} channels, and are not shown to scale. (B) A stylized view of a Ca^{2+} channel, from the extracellular side. The four P loops form a central pore, and the S4 segments are near the protein–lipid interface, by analogy to the bacterial K^+ channel structure (Jiang *et al.*, 2003a). Intracellular and extracellular connecting loops are not shown. (C) A kinetic model for channel gating (Kuo and Bean, 1994; Serrano *et al.*, 1999). The numerical subscripts give the number of voltage sensors (S4's) in the activated position. As described in the text, this model assumes that all four voltage sensors must activate before the channel can open, but inactivation can occur directly from closed states. The horizontal steps are voltage-dependent, while the vertical steps (inactivation and recovery) depend not on voltage directly but on the number of activated voltage sensors. The thickness of the vertical arrows is based on models for T-channel gating (Frazier *et al.*, 2001; Serrano *et al.*, 1999). Note that the inactivation rate is assumed to be maximal with only three of the four voltage sensors activated. The main pathways for channel activation, inactivation, and recovery from inactivation are indicated.

(Thévenod and Jones, 1992). The structural basis remains to be explored.

The data with Cd^{2+} also raise the issue of whether a closed channel is really fully closed. If Cd^{2+} can get in and out of a closed channel, albeit at 100-fold lower rates than when the channel is open, could the same be true for Ca^{2+}? A steady Ca^{2+} influx through "closed" channels at the resting potential of a cell could have significant consequences for regulation of intracellular Ca^{2+}. If the conductance of a "closed" channel were 1% of the open-channel conductance, that would be undetectable at the single-channel level, but the resulting whole-cell current should be detectable upon blockade by an appropriate channel blocker. For comparison, a closed K^+ channel has a low but detectable conductance, about 10^{-5} that of the open channel (Soler-Llavina *et al.*, 2003).

Where Are the Inactivation Gates?

During maintained depolarization, Ca^{2+} channels tend to inactivate, but the rate and extent of inactivation vary dramatically. In general, Ca^{2+} channels can inactivate by either Ca^{2+}-dependent or voltage-dependent mechanisms (Budde *et al.*, 2002; Eckert and Chad, 1984; Hering *et al.*, 2000; Stotz and Zamponi, 2001). Ca^{2+}-dependent inactivation is the dominant process for the $\alpha 1$C L-type channel of cardiac and smooth muscle, but may also occur for other high voltage-activated (HVA)

channels, usually more slowly. Ca^{2+}-dependent inactivation is a calmodulin-dependent process, involving sites on the C-terminal domain of the channel (Peterson *et al.*, 1999; Zühlke *et al.*, 1999). How Ca^{2+} binding is coupled to inactivation of the channel is not known. In some conditions, for some channels, Ca^{2+} binding can actually increase the current: facilitation (DeMaria *et al.*, 2001; Zühlke *et al.*, 1999).

"Voltage-dependent" inactivation is a grab-bag term for inactivation that does not obviously depend on Ca^{2+}. T-type Ca^{2+} channels tend to inactivate rapidly and almost completely (Perez-Reyes, 2003; Yunker and McEnery, in press), but inactivation of HVA channels tends to be slow, incomplete, and multiexponential. Voltage-dependent inactivation of HVA channels can be powerfully modulated by Ca^{2+} channel β subunits (Dolphin, in press), and in some cases by phosphorylation. A single N-channel can spontaneously switch between inactivating and noninactivating modes, perhaps reflecting modulation by some cellular signalling process (Plummer and Hess, 1991). At the whole-cell level, inactivation of N-current was described by the sum of two exponentials plus a third (apparently noninactivating) component; treatment with the phosphatase inhibitor okadaic acid induced an additional rapidly inactivating component (Werz *et al.*, 1993). It is not clear whether each exponential component reflects a distinct molecular mechanism of inactivation, which complicates interpretation of structure-function studies. Mutations in a variety of locations in the $\alpha 1$ subunits of Ca^{2+} channels can modify voltage-dependent inactivation (Berrou *et al.*, 2001; Hering *et al.*, 1998; Soldatov, 2003; Stotz and Zamponi, 2001; Zhang *et al.*, 1994). These studies have not led to the clear identification of an inactivation gate, although the loop between domains I–II is a candidate (Stotz and Zamponi, 2001). If results on voltage-dependent K^+ channels are a lesson for Ca^{2+} channels, there are likely to be a variety of mechanisms underlying voltage-dependent inactivation (Hoshi *et al.*, 1990; Klemic *et al.*, 2001; Liu *et al.*, 1996).

One clear-cut result from structure–function studies is negative: inactivation is not slowed by transplantation of the intracellular domain connecting domains III–IV from a slowly inactivating L-channel to a rapidly inactivating T-channel (Staes *et al.*, 2001). This distinguishes T-channel inactivation from fast inactivation of Na^+ channels, which depends critically on the structure of the III–IV linker (Stühmer *et al.*, 1989; West *et al.*, 1992).

How Are the Voltage Sensors Coupled to the Gates?

As discussed above, the structure of a Ca^{2+} channel $\alpha 1$ subunit immediately suggests an allosteric gating mechanism, since four distinct voltage sensors must cooperate to gate a single pore. This argument applies both to activation and to inactivation. The simplest model is that all four voltage sensors must move before the channel can open or inactivate. That is often assumed to be true for activation, as in *Shaker* K^+ channels (Zagotta and Aldrich, 1990), although some Ca^{2+} channels may be able to open before all voltage sensors activate (Lacinova *et al.*, 2002; Marks and Jones, 1992). Also, some Ca^{2+} channels are clearly able to inactivate from closed states (Patil *et al.*, 1998). Perhaps channels can inactivate with any number of activated voltage sensors, but activation of each voltage sensor favors inactivation (Kuo and Bean, 1994). One specific scheme is based on the classical MWC model for allosteric activation of an enzyme (Monod *et al.*, 1965), where activation of a voltage sensor is analogous to binding of a substrate molecule, and channel inactivation is analogous to enzyme activation (Fig. 2(C)).

The simplest version of an allosteric model assumes that the four voltage sensors have identical effects. That is appropriate as a "null hypothesis," but the four internally homologous domains of a Ca^{2+} or Na^+ channel are not identical in amino acid sequence, so they could be functionally different as well (either quantitatively or qualitatively). There is increasing evidence for this. T-channel inactivation reaches a maximal rate at voltages where only about half of the channels are open, suggesting that one or more voltage sensors are coupled weakly if at all to inactivation (Frazier *et al.*, 2001). The voltage sensor in domain IV appears to be especially strongly coupled to inactivation of Na^+ channels (Chen *et al.*, 1996).

Formally speaking, allosteric coupling between voltage sensors and gates is a mechanism, but it does not define a *molecular* mechanism. One interpretation is a truly allosteric process, where the positions of the voltage sensors modulate the equilibrium between two global conformations of the channel protein. However, it is equally consistent with other physical processes. Consider a ball-and-chain inactivation mechanism, like N-type inactivation of a K^+ channel. Suppose that the factor that makes the channel a good receptor for the ball is not channel opening, but outward movement of the positively charged voltage sensors, which would favor binding of a positively charged ball to the intracellular side of the channel (Patlak, 1991).

The crystal structure of a bacterial voltage-dependent K^+ channel suggests (but does not prove) one simple mechanism for coupling of the voltage sensors to the pore. The outward movement of the voltage-sensor paddle pulls on the S4–S5 linker, which in turn pulls on the cytoplasmic gate of the channel (Jiang *et al.*, 2003b).

Classically, activation and inactivation gates are distinct entities. That is most dramatically demonstrated

by the actions of intracellular proteases, which remove forms of voltage-dependent inactivation from Na^+ channels (Armstrong *et al.*, 1973; Rudy, 1978), *Shaker* K^+ channels (Hoshi *et al.*, 1990), and L-type Ca^{2+} channels of smooth muscle (Obejero-Paz *et al.*, 1991). In those studies, proteases did not affect channel activation, or certain other inactivation processes (slow inactivation of the Na^+ and K^+ channels, or voltage-dependent inactivation of L-channels). For *Shaker* K^+ channels, there appear to be at least three distinct gates, for activation (intracellular portion of S6), fast inactivation (N-terminal ball-and-chain), and slow inactivation (a conformational change in the outer mouth of the pore). It seems likely that Ca^{2+} channels also have multiple gates.

PERMEATION

Are Bacterial K^+ Channels Good Models for the Ca^{2+} Channel Pore?

As discussed above, the crystal structures of bacterial K^+ channels have revealed mechanisms of voltage sensor movement and activation gating that are likely to be conserved among voltage-dependent cation channels. However, it is not yet clear whether bacterial K^+ channels inactivate by mechanisms conserved with eukaryotic channels (Ruta *et al.*, 2003). Regarding permeation, there are two reasons to be pessimistic about the direct applicability of the K^+ channel structure to the Ca^{2+} channel pore: a low degree of sequence conservation in the P loop (Fig. 3), and evidence for different mechanisms of ion selectivity.

The K^+ channel selectivity filter consists primarily of the carbonyl groups from the backbone of the polypeptide chain in the GYG region of the pore loop (Doyle *et al.*, 1998). This selects for monovalent cations by providing a polar environment with a partial negative charge, and is just the right diameter to select for K^+ over cations of different size. In contrast, the crucial feature of the Ca^{2+} channel pore is a ring of four negative charges (Heinemann *et al.*, 1992; Yang *et al.*, 1993). In HVA channels, each of the four P loops contains a glutamate; in LVA channels, there are two glutamates and two aspartates at the corresponding position (*, Fig. 3). Many of the features of Ca^{2+} channel selectivity can be explained by the pore acting simply as an ion exchange resin, with the four closely spaced negative charges attracting an equal number of positive charges (Nonner and Eisenberg, 1998). The high density of negative charge in the pore is crucial for selectivity for divalent cations. Indeed, in the absence of divalents, Ca^{2+} channels are nonselective cation channels that allow even relatively large organic cations to permeate (McCleskey and Almers, 1985). In summary, Ca^{2+} channels (and Na^+ channels) select for their preferred ion using functional groups on the side chains of amino acids in the P loop, while K^+ channels use backbone carbonyls.

Although the functional groups involved in ion selectivity differ, the overall structure of the P loop may be conserved, acting as a module that can be customized by evolution to select for different ions (MacKinnon, 1995). Indeed, the bacterial K^+ channel structure has been used as a basis for molecular models of the Na^+ and Ca^{2+} channel pores (Lipkind and Fozzard, 2000, 2001). Testing this idea will require structural information on Ca^{2+} and/or Na^+ channels.

FUNCTION

Are Protein–Protein Interactions Fundamental to Ca^{2+} Channel Function?

It is said that there are "six degrees of separation" among humans: any two people can be connected by a short chain of common acquaintances. Proteins are like that, too. It seems likely that a brief list of pairwise protein–protein interactions could link any two proteins in a cell. Ca^{2+} channels are no exception. But why is this? If the main ($\alpha 1$) subunit of a Ca^{2+} channel is sufficient to produce Ca^{2+} entry, why should evolution have allowed other proteins to interfere with this elegant mechanism?

Classically, Ca^{2+} channels have several subunits (distinguished by Greek letters), originally identified by biochemical purification procedures for the Ca^{2+} channel of skeletal muscle: $\alpha 1$, $\alpha 2/\delta$, β, and γ. Classically, these are thought to be invariant, stoichometrically-associated proteins. Many studies have examined the effects of the "accessory" subunits on $\alpha 1$, either at the level of membrane expression of functional Ca^{2+} channels, or modulatory effects on channel electrophysiology (Black, in press; Dolphin, in press; Klugbauer *et al.*, in press).

Functional expression of $\alpha 1$ subunits can occur in the nominal absence of accessory subunits, but one study found that antisense against β subunits prevented functional expression of $\alpha 1$ in *Xenopus* oocytes, revealing a role for β subunits expressed endogenously by the oocyte (Tareilus *et al.*, 1997). This led to the idea that β subunits act as a chaperones, enhancing expression of the $\alpha 1$ subunit in the plasma membrane (Herlitze *et al.*, in press). However, β subunits have additional actions on Ca^{2+} channel gating (Dolphin, in press), suggesting either that the initial $\alpha 1$–β interaction is transient, or perhaps more likely, that a second β subunit can bind reversibly to the $\alpha 1$–β complex. So are β subunits really subunits,

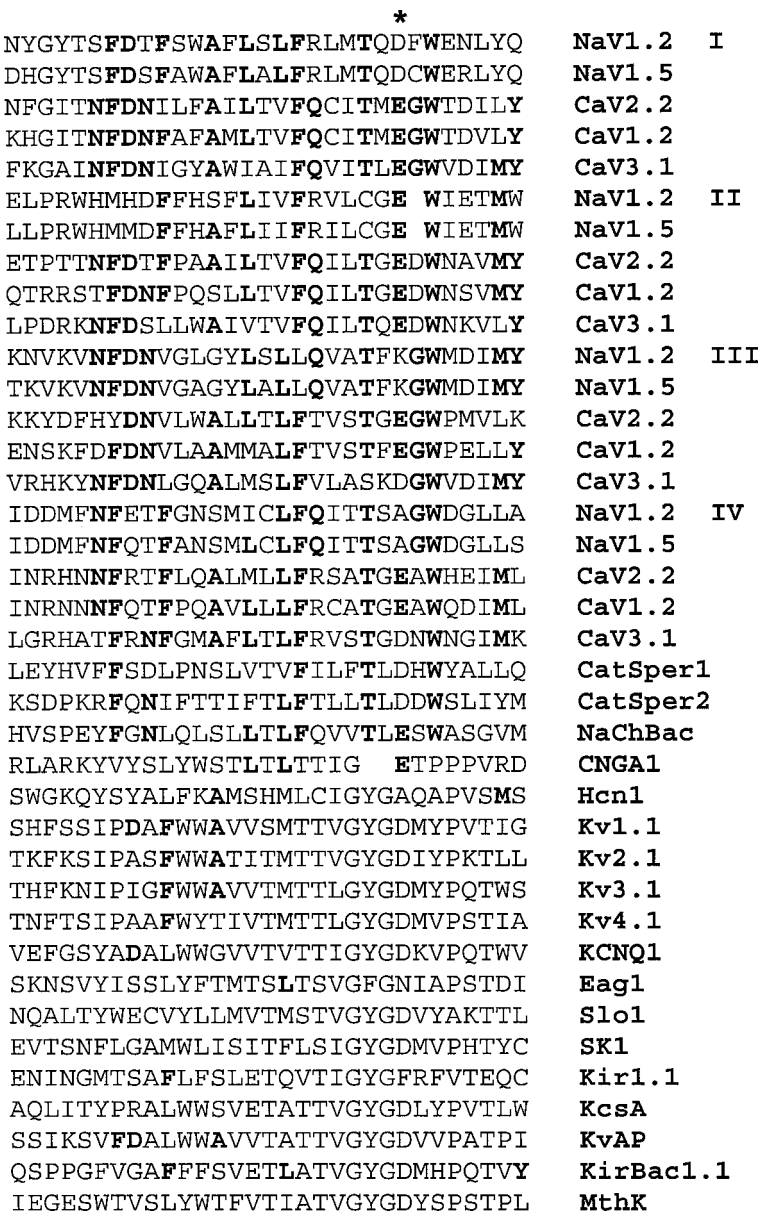

Fig. 3. Alignment of the P loops of representative channels. At the top, two Na^+ channels and three Ca^{2+} channels are shown, including the P loops from each of the four domains. Note that conservation is stronger across channels within a domain, than within a channel across domains, as expected if Na^+ and Ca^{2+} channels originated from a common ancestor by duplication of a single domain (Hille, 2001). The site critical for ion selectivity in Ca^{2+} and Na^+ channels is marked (*). Amino acids present in at least half of the four-domain Na^+ and Ca^{2+} channel P loops are highlighted in bold. Note that those are rarely present in K^+ channels. This alignment includes a two amino acid deletion in cyclic nucleotide-gated channels (Heginbotham *et al.*, 1992), but *not* in Na^+ and Ca^{2+} channels. Species, and GenBank GI numbers: NaV1.2 (human, 457879), NaV1.5 (human, 184039), CaV2.2 (human, 179758), CaV1.2 (human, 463079), CaV3.1 (human, 3786351), CatSper1 (human, 16076816), CatSper2 (human, 16566356), NaChBac (*Bacillus halodurans*, 10174118), CNGA1 (human, 180462), Hcn1 (mouse, 3242242), Kv1.1 (rat, 206491), Kv2.1 (rat, 57786), Kv3.1 (rat, 205107), Kv4.1 (mouse, 199813), KCNQ1 (human, 2465515), Eag1 (rat, 557265), Slo1 (mouse, 347144), SK1 (human, 1575661), Kir1.1 (rat, 296619), KcsA (*Streptomyces lividans*, 1089906), KvAP (*Aeropyrum pernix*, 5104624), KirBac1.1 (*Burkholderia pseudomallei*; no GenBank entry, see http://www.sanger.ac.uk/Projects/Microbes/), MthK (*Methanothermobacter thermautotrophicus*, 2622639).

or just proteins that happen to modulate Ca^{2+} channels (Jones, 2002)?

These issues recur for γ subunits (Black, in press; Qiao and Meng, in press). Initially, only a single $\gamma 1$ subunit was known, associated with $\alpha 1S$ but not other Ca^{2+} channels. More recently, a family of related proteins have been identified ($\gamma 2$–$\gamma 8$), some of which are known to be associated with neuronal Ca^{2+} channels and/or to modulate their functional properties. However, $\gamma 2$ is also associated with the AMPA-type glutamate receptor (Chen *et al.*, 2000), challenging its identity as a Ca^{2+} channel subunit. This controversy is reviewed in more detail by Black (in press) and Qiao and Meng (in press). Another possibility is that the γ subunits are scaffolding and/or cytoskeletal proteins involved in localization of multiple transmembrane proteins, including Ca^{2+} channels.

One clear example where protein–protein interactions are critical for function is the role of $\alpha 1S$ in excitation–contraction coupling in skeletal muscle (Franzini-Armstrong and Protasi, 1997). Although $\alpha 1S$ does form a functional Ca^{2+} channel, it activates quite slowly, too slowly to provide significant Ca^{2+} influx on the time scale of a single muscle action potential (Sanchez and Stefani, 1983). Instead, $\alpha 1S$ acts as the voltage sensor for release of Ca^{2+} from the sarcoplasmic reticulum, via the ryanodine receptor Ca^{2+} channel. Domains critical for this process have been identified (Grabner *et al.*, 1999; Nakai *et al.*, 1998; Protasi *et al.*, 2002), so it is likely but still not certain that the $\alpha 1S$-ryanodine receptor interaction is direct. Is this a specialized property of $\alpha 1S$, or is this just the first example of a "Ca^{2+} channel" acting as a signalling molecule, in a manner independent of Ca^{2+} influx? There is some evidence for functional coupling of neuronal L-channels to ryanodine receptors (Chavis *et al.*, 1996).

In addition to the classical accessory subunits, Ca^{2+} channels interact with a variety of other proteins, including syntaxin (Bezprozvanny *et al.*, 1995; Sheng *et al.*, 1994), calmodulin (Zühlke *et al.*, 1999), and the $\beta\gamma$ subunits of G proteins (Elmslie, in press; Herlitze *et al.*, 1996; Ikeda, 1996;). Are these interactions strong enough that we should consider these proteins to also be subunits of Ca^{2+} channels? The case may be strongest for calmodulin, which is associated with Ca^{2+} channels even in the absence of elevated Ca^{2+}, although the interaction is sufficiently reversible for overexpressed calmodulin mutants to displace native calmodulin (Peterson *et al.*, 1999).

To this point, the discussion of Ca^{2+} channel subunits has really considered only HVA channels. T-channels are fully functional electrophysiologically when the $\alpha 1$ subunit is expressed nominally alone in *Xenopus* oocytes or mammalian cell lines (Perez-Reyes, 2003), but coexpression with the accessory subunits of HVA channels sometimes has modest effects (Dolphin *et al.*, 1999; Green *et al.*, 2001; Klugbauer *et al.*, 2000; Lacinova *et al.*, 1999; Yunker and McEnery, in press).

To summarize the question I wish to raise here: Are protein–protein interactions are fundamental to the physiological function of Ca^{2+} channels (other than $\alpha 1S$), or is this simply another layer of complexity for Ca^{2+} channel regulation? This question applies both to the proteins classically identified as Ca^{2+} channel subunits, and to other proteins such as calmodulin and syntaxin.

Do Voltage-Dependent Ca^{2+} Channels Regulate Basal Intracellular Ca^{2+}?

One of the many things about biology that is difficult to explain to a physicist is that facts can have the impact of concepts. The all-or-none signalling provided by action potentials is surely a concept, but this depends on the contingent facts that the ion gradients for Na^+ and K^+ are in opposite directions, and that voltage-dependent ion channel proteins have evolved to exploit this. Similarly, the unique role of Ca^{2+} as a signalling molecule depends on the fact that $[Ca^{2+}]_i$ is remarkably low, $\sim 10^{-7}$ M, at least four orders of magnitude lower than the other physiologically prevalent inorganic ions. Since $[Ca^{2+}]_o$ is $\sim 10^{-3}$ M, opening of a relatively small number of Ca^{2+} channels can cause large ($\sim$10-fold) changes in $[Ca^{2+}]_i$. This allows cells to variously interpret changes in $[Ca^{2+}]_i$ as signals for secretion, contraction, gene expression, life, and death.

Many processes regulate intracellular Ca^{2+}, including cytoplasmic Ca^{2+} binding proteins and uptake into organelles, but at steady-state it is the balance between Ca^{2+} influx and efflux at the plasma membrane that determines $[Ca^{2+}]_i$ (Friel, 1995). Mechanisms for Ca^{2+} efflux (against the strong electrochemical gradient) include Na^+-Ca^{2+} exchange and ATP-dependent Ca^{2+} pumps, which will not be considered further here. Ca^{2+} influx occurs through both voltage-dependent Ca^{2+} channels, and a variety of other Ca^{2+}-permeable channels. In particular, the large family of Trp-related Ca^{2+} channels includes candidates for regulation of $[Ca^{2+}]_i$ (Benham *et al.*, 2002; Montell *et al.*, 2002; Voets and Nilius, 2003).

How can voltage-dependent Ca^{2+} channels, which tend to be closed at resting membrane potentials, contribute to basal $[Ca^{2+}]_i$? One speculative mechanism is that the "closed" channel has a nonzero conductance to Ca^{2+} (see above). The more classical mechanism is a "window current," resulting from overlap of the activation and inactivation curves (Fig. (4)A). There can be a

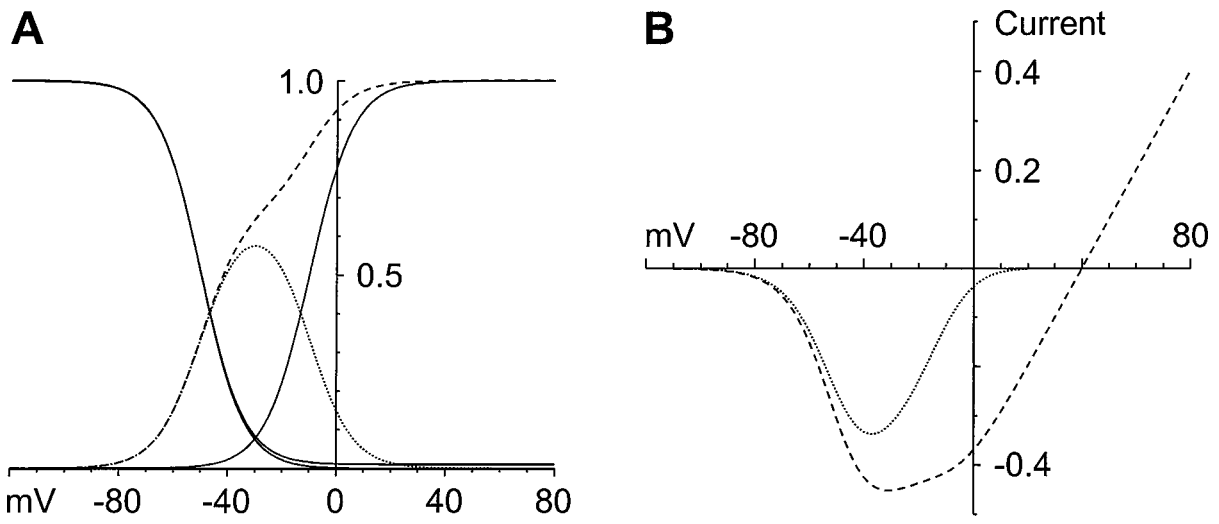

Fig. 4. Window currents and "open window currents." (A) The solid curves are hypothetical activation and inactivation curves for a Ca^{2+} channel, described by Boltzmann relations with midpoint voltages −10 and −50 mV (respectively), and slope factors of 8 mV. Two inactivation curves are shown, extrapolating to 99% or 100% inactivation at extreme positive voltages. If activation and inactivation are independent (see text!), multiplication of the activation × inactivation curves gives the steady-state p(open). That is shown as the dashed curve (for 99% inactivation) and the dotted curve (for 100% inactivation), on a 100-fold expanded scale (i.e., 1.0 =1%). (B) Predicted steady-state currents, assuming a linear open-channel I–V with a reversal potential of +40 mV and a maximal conductance of 1.0 (arbitrary units). The dashed line is the "open window current" (maximal inactivation 99%), and the dotted line is the classical window current (maximal inactivation 100%). In the absence of inactivation, the peak inward current would be −19.8, at −3 mV.

voltage region where channels are partially activated, but not fully inactivated, predicting a steady-state current.

The calculation of the window current begins by multiplying the activation curve × the inactivation curve, to get the steady-state open probability. There are at least three problems with this. First, the activation curve is often measured inappropriately. Second, the inactivation curve is often measured inappropriately. Third, multiplying the two curves is not valid. Explanation of these problems will require a rather long biophysical digression. The take-home message is that activation and inactivation curves (or window currents) are not as easy to measure accurately as might be thought.

Measurement of Activation Curves

Sometimes activation curves are calculated from "chord conductances" using the equation $I = G(V - V_R)$, where I is the experimentally observed current at voltage V, G is the chord conductance, and V_R is the reversal potential for the channel of interest (Hodgkin and Huxley, 1952b). However, G is proportional to the channel open probability only if the single channel conductance is independent of voltage: i.e., the open channel behaves like a resistor (Hodgkin and Huxley, 1952a). In principle, Ca^{2+} channels are especially unlikely to obey this rule, since the extremely strong transmembrane Ca^{2+} gradient should produce strong rectification (Fig. 4.18 of Hille, 2001). This is nicely illustrated by data on the α1G T-type Ca^{2+} channel (Fig. 5). Following maximal activation, inward currents (carried by Ca^{2+}) are relatively large, outward currents (carried by Na^+ in these experimental conditions) are very large, but the I–V flattens noticeably near the reversal potential, where ion–ion competition limits flux (open symbols, Fig. 5(A)). This nonlinear "instantaneous" I–V implies that the conductance of a single open channel depends on voltage. When peak currents are measured upon direct depolarization (solid symbols, Fig. 5(A)), the calculated chord conductance exhibits a bizarre voltage-dependence (solid symbols, Fig. 5(B)), which approximates the expected Boltzmann relationship only at negative voltages. The peak p(open) is proportional to the *ratio* of the "standard" to the "instantaneous" conductance, not to the standard conductance alone (Serrano *et al.*, 1999).

Theoretically, a simple Boltzmann relationship is expected to accurately describe the activation curve only if a channel obeys simple two-state (C⇌O) kinetics, *and* if the rate constants for channel opening and closing depend exponentially and symmetrically on voltage. As an example, the activation curve for a Hodgkin and Huxley (1952c)

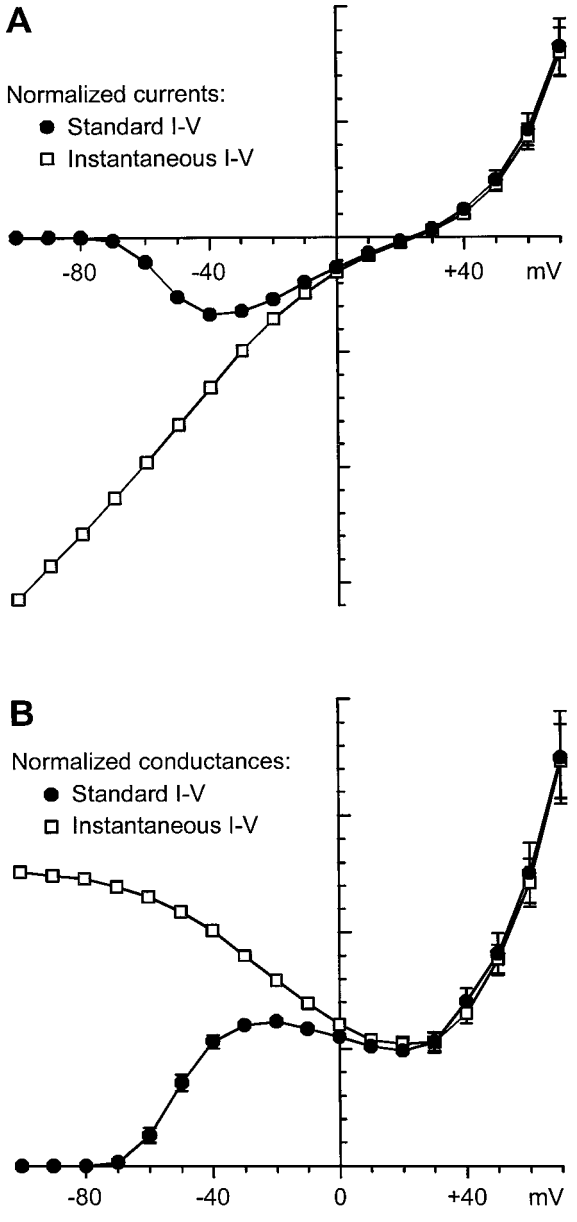

Fig. 5. Currents and conductances for the α1G T-channel. (A) Current–voltage (I–V) relations. Data are from two protocols, the "standard" I–V (measuring the peak current during depolarization from −100 mV to the indicated voltage), and the "instantaneous" I–V (the current measured immediately after repolarization to the indicated voltage, following a 2 ms step to +60 mV, which produces maximal channel activation with little inactivation). The "instantaneous" current equals the single-channel current × the number of channels opened at +60 mV. Data are from the study of Serrano *et al.* (1999), $n = 6$. To reduce variability from different channel expression levels among cells, values were normalized to the sum of the absolute values of all currents from the instantaneous I–V from −100 to +60 mV, so the vertical scale is arbitrary. (B) Conductances were calculated from the normalized currents using the chord conductance equation, $G = I/(V - V_R)$, where V_R is the observed reversal potential in each cell ($+25 \pm 2$ mV). Note that the open-channel conductance varies > 3-fold over the voltage range examined (open symbols).

K^+ channel deviates from a pure Boltzmann relationship both because of the n^4 behavior (all four voltage sensors must be activated for the channel to open), and because the rate constant for channel activation does not depend exponentially on voltage. For voltage-dependent K^+ channels, complex activation curves are observed experimentally, and also predicted from detailed models for channel activation (Klemic *et al.*, 1998; Schoppa and Sigworth, 1998; Zagotta *et al.*, 1994). Even when a Boltzmann-based fit gives a reasonable description of the overall activation curve, it often misses the data points at the "foot" of the activation process where p(open) is low, which are most crucial for estimation of a window current.

For a channel that inactivates, measurement of the activation curve is problematic. (Remember that the goal is the steady-state probability that the channel is open, considering only the channel activation process.) The peak current at a particular voltage can be affected by inactivation, if some channels inactivate before the current reaches its maximal value. Even worse, the fraction of channels that inactivate prior to the peak will vary with voltage. When inactivation is prevented (e.g., by treating Na^+ channels with intracellular proteases), large shifts in the activation curve can be revealed (Cota and Armstrong, 1989; Gonoi and Hille, 1987).

Measurement of Inactivation Curves

There are three typical problems with "steady-state" inactivation curves. First, inactivation curves are often measured at an arbitrarily chosen time, with no evidence that inactivation has reached a steady-state. Second, many voltage-dependent channels exhibit very slow inactivation processes. Slow inactivation may be missed entirely on the time scale of typical electrophysiological experiments, or it may contribute in a poorly defined manner to the measured inactivation. Third, some channels may not inactivate completely.

In principle, for a single well-defined inactivation process, it is simple to determine when inactivation is at steady-state (Jones, 1987; Serrano *et al.*, 1999). Measure the time course of inactivation at each voltage, and compare that to the time course of recovery from inactivation at the same voltage. (This of course makes sense only in the middle of the inactivation curve, where between 0 and 100% of the channels are available at steady-state.) If the two protocols give the same final % inactivation, then the channel has "forgotten" the initial conditions, and inactivation has reached steady-state. Since the time constant for inactivation is typically the slowest at voltages near 50% inactivation, the rate of inactivation at strongly depolarized

voltages may greatly underestimate the time required to reach steady-state elsewhere.

Even if inactivation passes this test for steady-state, many voltage-dependent channels exhibit separate slow inactivation processes (sometimes called "ultra slow"), on the time scale of many seconds or minutes. This has been characterized most thoroughly for Na^+ channels (Cummins and Sigworth, 1996; Rudy, 1978), but is also known for L-type (Schouten and Morad, 1989) and N-type (Degtiar *et al.*, 2000; Jones and Marks, 1989b) Ca^{2+} channels. Slow inactivation can strongly limit channel availability near the resting potential of a cell.

It is often assumed that inactivated states are "absorbing," i.e., that inactivation reaches 100% at sufficiently depolarized voltages. This may not be true for Ca^{2+} channels. Even for T-channels, which inactivate more strongly than most other Ca^{2+} channels, 1–2% of the channels may remain open at steady-state (Frazier *et al.*, 2001; Serrano *et al.*, 1999). This small residual component can easily be missed when an inactivation curve is fitted to a Boltzmann function (Fig. 4(A)). The steady-state current resulting from incomplete inactivation has a wider voltage-dependence than a classical window current, where there is a significant steady-state p(open) only in the narrow voltage window where the activation and inactivation curves overlap (Fig. 4(B)). I propose that the steady-state current resulting from incomplete inactivation be called an "open window current."

Measurement of Window Currents

Finally, even if activation and inactivation curves are measured accurately, multiplying the two curves point-by-point gives the steady-state p(open) only if activation and inactivation are independent (since independent probabilties multiply). That is true for classical models of inactivation (Hodgkin and Huxley, 1952c), but it is now clear that activation and inactivation are kinetically coupled. Given all of the problems detailed above, it is best to consider this calculation as a basis for *prediction* of a window current, rather than as a direct experimental *measurement*.

Why not measure the window current directly? Sometimes that can be done, e.g., detecting a persistent Na^+ current as a TTX-sensitive difference current (French *et al.*, 1990). However, window currents are generally small, and their direct measurement is prone to error from leak subtraction and other technical problems. One possibility is to quickly hyperpolarize, to detect ongoing channel activity as a tail current. For Ca^{2+}, the increased driving force at hyperpolarized voltages will enhance the signal-to-noise ratio, at least if the tail current is relatively slow, as for T-type Ca^{2+} channels (Serrano *et al.*, 1999). A caveat is that if the window current is very small, it is necessary to distinguish an ionic tail current from an "off" gating current (Burgess *et al.*, 2002).

Incomplete inactivation of Ca^{2+} channels is also crucial for the effect of high K^+ to raise intracellular Ca^{2+}, either experimentally, or in pathological conditions such as epilepsy where extracellular K^+ is elevated. Biochemists seem to think that depolarizing cells by addition of extracellular K^+ is a simple experiment, but electrophysiologists find this extremely difficult to interpret. The residual Ca^{2+} channel activity following minutes or hours of depolarization cannot be predicted directly from typical electrophysiological experiments, where depolarizations rarely exceed a few seconds. Slow inactivation processes, which are known to exist (as noted above) but are generally poorly characterized, will have a dominant effect. Experimentally, inactivation of L-channels may be less complete than other HVA channels (Marchetti *et al.*, 1995). One candidate is the α1D L-channel, which activates at somewhat more negative voltages than other HVA channels (Koschak *et al.*, 2001; Xu and Lipscombe, 2001).

Are N and P/Q Channels Specialized for Rapid Transmitter Release?

The discovery of multiple calcium channel types, based first on electrophysiological evidence and later on molecular studies (Fig. 1), led to the obvious speculation that channels are specialized for different functions. The radically different gating kinetics of HVA vs. LVA channels supported that hypothesis, and it is clear that LVA (T-type) channels play specialized functional roles (Perez-Reyes, 2003; Yunker and McEnery, in press). However, the situation is less clear-cut among HVA channels. L-type channels are expressed in muscle, where they are crucial for regulation of muscle contraction, but they are also widespread in neurons and other secretory cells. Other HVA channels (notably N and P/Q channels) seem to be restricted to neurons and related endocrine cells, and are certainly the primary Ca^{2+} channels involved in the release of neurotransmitters at most synapses (Dunlap *et al.*, 1995). But why is that? What properties of N and/or P/Q channels adapt them for this function?

For an electrophysiologist, the first place to look for specialized channel properties is differences in gating kinetics (activation and inactivation). Qualitatively, however, all HVA channels (with the exception of α1S) behave similarly upon strong depolarization, activating in $\sim$1 ms, and closing in < 1 ms upon repolarization. Thus, the activation kinetics of HVA channels are intermediate between fast Na^+ channels and slow LVA channels.

Under voltage-clamp, the mean open time of a simply behaved channel is random, exponentially distributed. This biophysical property threatens to severely impact the reliability of neurotransmitter release, since an exponential distribution is highly variable: most open durations are brief, but some are quite long, and the standard deviation equals the mean! This would make the Ca^{2+} influx through a single channel extremely variable.

Consider instead the response of HVA channels to a typical brief action potential, the physiological signal for synchronous release of neurotransmitter from a nerve terminal (Sabatini and Regehr, 1999). As the voltage goes rapidly from the resting potential (where HVA channels are closed) to the peak of the action potential (+40 mV), HVA channels will begin to open (Fig. 6). During repolarization, the increase in driving force on Ca^{2+} will generate

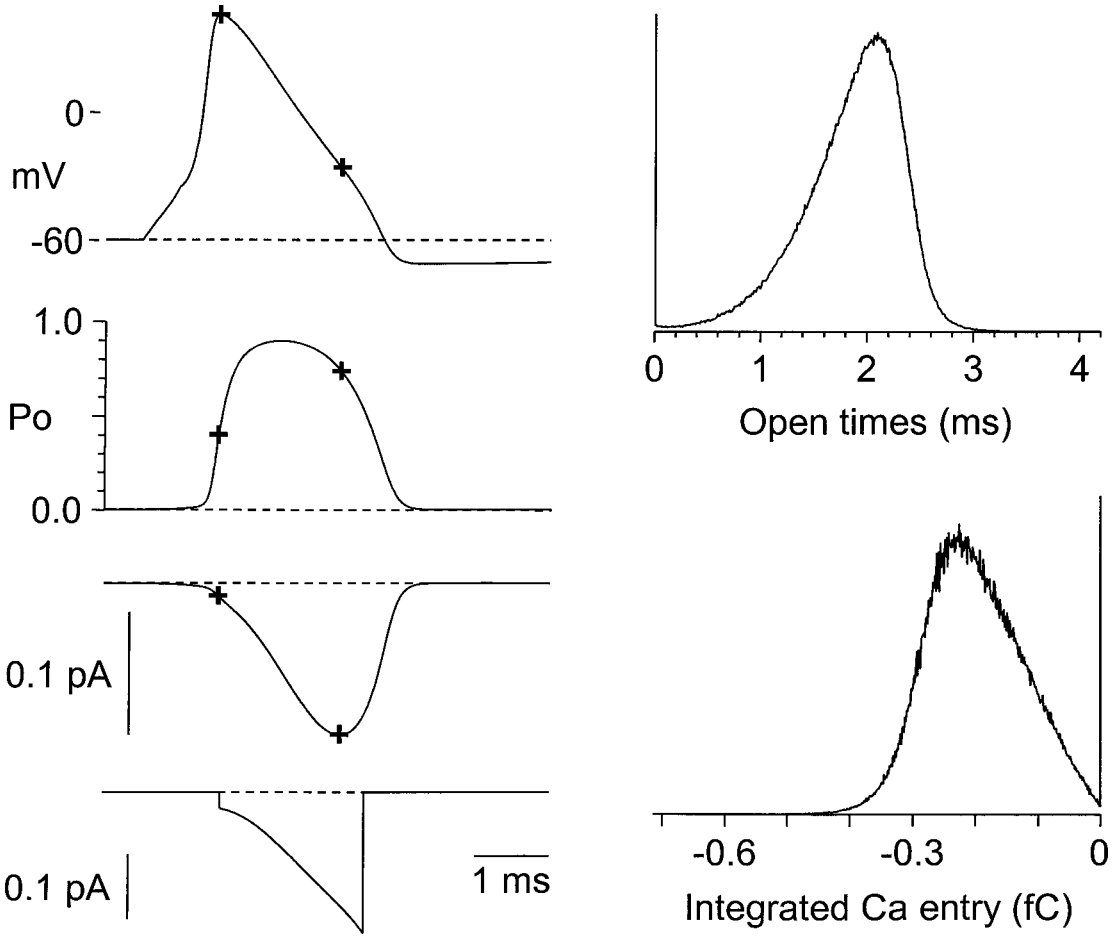

Fig. 6. Simulation of calcium channel activation during an action potential, based on a two-state C−O model for N-channel gating (Jones and Marks, 1989a). The left column (top to bottom) shows the simulated action potential (Hodgkin and Huxley, 1952c), the average calcium channel open probability, the average calcium channel current, and a "typical" single calcium channel record (with the median observed latency, and median open duration). The "+" signs in the top three panels mark the time of the action potential peak and of the peak calcium current. Note that the Ca^{2+} current flows almost entirely during repolarization of the action potential. The right column shows the distributions of calcium channel open times (above) and of net Ca^{2+} entry (below) (1 fC = 3120 Ca^{2+} ions). For 7.3% of the action potentials, the calcium channel did not open (reflected in the truncated vertical lines at zero in the right panels). Channel gating was simulated using a Monte Carlo method (Bennett *et al.*, 1997), in response to 10^6 action potentials. Calcium current through a single open channel was described by the Goldman–Hodgkin–Katz current equation with a voltage offset (Bennett *et al.*, 1997). The single channel current was reduced by a factor of 7 from Bennett *et al.* (1997), which was based on single channel data in 110 mM Ba^{2+}. Data on the conductance of single N or P/Q channels in 2 mM Ca^{2+} does not seem to be available, so the estimate here is based on L-channels (Church and Stanley, 1996; Guia *et al.*, 2001; Rubart *et al.*, 1996).

a strong inward Ca^{2+} current, but the channels will then quickly close. Thus, an action potential can help synchronize channel opening and closing, which greatly reduces variability in channel open times and in the resulting Ca^{2+} entry per channel (Fig. 6).

It is believed that Ca^{2+} influx in response to an action potential is effectively a "tail current," occurring primarily during repolarization (Llinas *et al.*, 1981a), although fast channel closing at 37°C could terminate Ca^{2+} influx rapidly (Sabatini and Regehr, 1996). The rising and falling phases of the action potential are comparable in duration to the time constants for activation gating of HVA channels, so the detailed kinetic properties of a channel can strongly affect its ability to supply Ca^{2+} for neurotransmitter release. The timing of channel closing is especially critical, since the driving force on Ca^{2+} is strong during repolarization of the action potential (see "typical" Ca^{2+} channel record, lower left panel of Fig. 6).

For comparison, action potential-evoked Ca^{2+} influx through a T-channel will reach a peak only after full repolarization, and will continue longer (McCobb and Beam, 1991; Scroggs and Fox, 1992), reflecting the slower channel closing (deactivation) characteristic of T-channels (Fig. 7).

Since neurotransmitter release is a faster process than muscle contraction, it might be expected that N and P/Q channels would activate more rapidly than L-channels. Curiously, the reverse seems to be true, although few studies appear to have examined this in detail. Roughly, the order appears to be $\alpha 1D > \alpha 1C > \alpha 1A > \alpha 1B$ (from faster to slower; again, excluding $\alpha 1S$). For the more slowly activating channels, a substantial fraction of channels may not open in response to one action potential (see Fig. 6).

How does inactivation affect the response of Ca^{2+} channels to an action potential? At first glance, inactivation seems much too slow to significantly affect Ca^{2+} entry in response to a $\sim$1 ms action potential, since the time constants for inactivation of HVA channels are $>$ 10 ms (often much greater). Although N and P/Q channels inactivate relatively slowly in response to long, maintained voltage steps, they exhibit strong cumulative inactivation in response to brief, repetitive action potential-like depolarizations, resulting from preferential inactivation from closed states (Patil *et al.*, 1998). This could contribute to synaptic plasticity during a train of action potentials.

In addition, inactivation controls the resting availability of Ca^{2+} channels. In addition to the relatively rapid inactivation visible during strong depolarizations, weak depolarizations can cause extremely slow inactivation, on a time scale of seconds to minutes (discussed above). Strikingly, interaction of Ca^{2+} channels with syntaxin can modulate slow inactivation (Degtiar *et al.*, 2000).

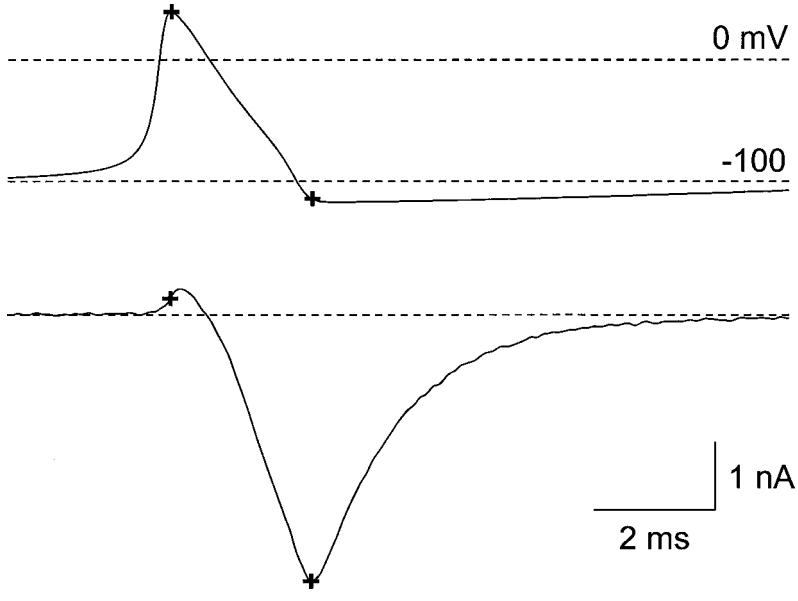

Fig. 7. Activation of T-current by an action potential waveform. Data are from cloned $\alpha 1G$ channels, expanded from Fig. 12B of Serrano *et al.* (1999). The simulated action potential used as the voltage command was scaled to begin from -100 mV, to prevent resting T-channel inactivation. The "+" signs mark the action potential peak, and the peak inward current. Compare to Fig. 6, a simulated N-channel.

If involvement of N and P/Q channels in transmitter release is the rule, it must be noted that there are exceptions. R-channels (Wu *et al.*, 1998), L-channels (Heidelberger and Matthews, 1992), and even T-channels (Pan *et al.*, 2001) can also mediate rapid neurotransmitter release. It is possible that the role of a calcium channel in neurotransmitter release is determined less by gating kinetics than by the channel's location. Perhaps the most important specializations of Ca^{2+} channels for transmitter release are their abilities to interact with presynaptic proteins. The efficacy of Ca^{2+} entry for evoking transmitter release depends on the type of channel through which the Ca^{2+} enters (Wu *et al.*, 1999), most likely resulting from differential localization of Ca^{2+} channels in or near the presynaptic active zone. Ca^{2+} channels can be modulated by some of the proteins involved in transmitter release, so Ca^{2+} channels at an active zone may function differently from Ca^{2+} channels in the cell body of a neuron, or recombinant Ca^{2+} channels in an expression system (Atlas, 2001; Jarvis and Zamponi, 2001; Stanley, 1997; Zhong *et al.*, 1999).

It has long been recognized that the submillisecond latency between the presynaptic action potential and the onset of neurotransmitter release strongly constrains the mechanism by which Ca^{2+} entry evokes release (Katz and Miledi, 1967; Llinas *et al.*, 1981b). There is simply no time for Ca^{2+} to do anything but diffuse a short distance (considerably less than 1 μm), bind to a target protein, and somehow trigger release. Diffusion calculations suggest that the local Ca^{2+} concentration approaches millimolar levels near the inner mouth of an open Ca^{2+} channel, but decreases steeply over tens of nanometers (Ríos and Stern, 1997). These transient "nanodomains" disappear within microseconds once the channel closes. All this is difficult to measure directly, but supporting evidence comes from the use of nearby Ca^{2+}-dependent K^+ channels as a bioassy for Ca^{2+} (Roberts *et al.*, 1990; Yazejian *et al.*, 2000), and from the effects of exogenous Ca^{2+} buffers. At the squid giant synapse, the fast Ca^{2+} buffer BAPTA inhibits release, but the slow buffer EGTA does not, consistent with rapid and highly localized Ca^{2+} action (Adler *et al.*, 1991). However, EGTA is effective at some synapses in the mammalian brain (Borst and Sakmann, 1996; Ohana and Sakmann, 1998), suggesting that the tightness of coupling of Ca^{2+} entry to exocytosis can vary, even among rapidly transmitting synapses. A related question is whether release from a vesicle depends on Ca^{2+} influx from a single nearby channel, or on the summed Ca^{2+} from multiple channels (Bertram *et al.*, 1996; Meinrenken *et al.*, 2003; Poage and Meriney, 2002).

In summary, the function of a Ca^{2+} channel in neurotransmitter release depends on an incompletely understood interplay between channel gating kinetics, and the channel's location and interactions within the molecular architecture of the presynaptic active zone.

ACKNOWLEDGMENT

Research in the author's laboratory is supported in part by NIH grant NS24471.

REFERENCES

Adler, E. M., Augustine, G. J., Duffy, S. N., and Charlton, M. P. (1991). *J. Neurosci.* **11**, 1496–1507.
Armstrong, C. M. (1971). *J. Gen. Physiol.* **58**, 413–437.
Armstrong, C. M., Bezanilla, F., and Rojas, E. (1973). *J. Gen. Physiol.* **62**, 375–391.
Atlas, D. (2001). *J. Neurochem.* **77**, 972–985.
Benham, C. D., Davis, J. B., and Randall, A. D. (2002). *Neuropharmacology* **42**, 873–888.
Bennett, M. R., Gibson, W. G., and Robinson, J. (1997). *Biophys. J.* **73**, 1815–1829.
Berrou, L., Bernatchez, G., and Parent, L. (2001). *Biophys. J.* **80**, 215–228.
Bertram, R., Sherman, A., and Stanley, E. F. (1996). *J. Neurophysiol.* **75**, 1919–1931.
Bezprozvanny, I., Scheller, R. H., and Tsien, R. W. (1995). *Nature* **378**, 623–626.
Black, J. L., III (2003). *J. Bioenerg. Biomembr.* **35**, 649–660.
Borst, J. G. G., and Sakmann, B. (1996). *Nature* **383**, 431–434.
Bourinet, E., Soong, T. W., Sutton, K., Slaymaker, S., Mathews, E., Monteil, A., Zamponi, G. W., Nargeot, J., and Snutch, T. P. (1999). *Nat. Neurosci.* **2**, 407–415.
Budde, T., Meuth, S., and Pape, H. C. (2002). *Nat. Rev. Neurosci.* **3**, 873–883.
Burgess, D. E., Crawford, O., Delisle, B. P., and Satin, J. (2002). *Biophys. J.* **82**, 1894–1906.
Chapman, M. L., VanDongen, H. M., and VanDongen, A. M. (1997). *Biophys. J.* **72**, 708–719.
Chavis, P., Fagni, L., Lansman, J. B., and Bockaert, J. (1996). *Nature* **382**, 719–722.
Chen, L., Chetkovich, D. M., Petralia, R. S., Sweeney, N. T., Kawasaki, Y., Wenthold, R. J., Bredt, D. S., and Nicoll, R. A. (2000). *Nature* **408**, 936–943.
Chen, L. Q., Santarelli, V., Horn, R., and Kallen, R. G. (1996). *J. Gen. Physiol.* **108**, 549–556.
Church, P. J., and Stanley, E. F. (1996). *J. Physiol.* **496**, 59–68.
Cota, G., and Armstrong, C. M. (1989). *J. Gen. Physiol.* **94**, 213–232.
Cummins, T. R., and Sigworth, F. J. (1996). *Biophys. J.* **71**, 227–236.
Degtiar, V. E., Scheller, R. H., and Tsien, R. W. (2000). *J. Neurosci.* **20**, 4355–4367.
Del Camino, D., Holmgren, M., Liu, Y., and Yellen, G. (2000). *Nature* **403**, 321–325.
DeMaria, C. D., Soong, T. W., Alseikhan, B. A., Alvania, R. S., and Yue, D. T. (2001). *Nature* **411**, 484–489.
Dolphin, A. C. (2003). *J. Bioenerg. Biomembr.* **35**, 599–620.
Dolphin, A. C., Wyatt, C. N., Richards, J., Beattie, R. E., Craig, P., Lee, J. H., Cribbs, L. L., Volsen, S. G., and Perez-Reyes, E. (1999). *J. Physiol.* **519**, 35–45.
Doyle, D. A., Cabral, J. M., Pfuetzner, R. A., Kuo, A. L., Gulbis, J. M., Cohen, S. L., Chait, B. T., and MacKinnon, R. (1998). *Science* **280**, 69–77.

Dunlap, K., Luebke, J. I., and Turner, T. J. (1995). *Trends Neurosci.* **18**, 89–98.
Eckert, R., and Chad, J. E. (1984). *Prog. Biophys. Mol. Biol.* **44**, 215–267.
Elmslie, K. S. (2003). *J. Bioenerg. Biomembr.* **35**, 477–490.
Ertel, E. A., Campbell, K. P., Harpold, M. M., Hofmann, F., Mori, Y., Perez-Reyes, E., Schwartz, A., Snutch, T. P., Tanabe, T., Birnbaumer, L., Tsien, R. W., and Catterall, W. A. (2000). *Neuron* **25**, 533–535.
Flink, M. T., and Atchison, W. D. (2003). *J. Bioenerg. Biomembr.* **35**, 697–713.
Franzini-Armstrong, C., and Protasi, F. (1997). *Physiol. Rev.* **77**, 699–729.
Frazier, C. J., Serrano, J. R., George, E. G., Yu, X., Viswanathan, A., Perez-Reyes, E., and Jones, S. W. (2001). *J. Gen. Physiol.* **118**, 457–470.
French, C. R., Sah, P., Buckett, K. J., and Gage, P. W. (1990). *J. Gen. Physiol.* **95**, 1139–1157.
Friel, D. D. (1995). *Biophys. J.* **68**, 1752–1766.
Gonoi, T., and Hille, B. (1987). *J. Gen. Physiol.* **89**, 253–274.
Grabner, M., Dirksen, R. T., Suda, N., and Beam, K. G. (1999). *J. Biol. Chem.* **274**, 21913–21919.
Green, P., Warre, R., Hayes, P., McNaughton, N., Medhurst, A., Pangalos, M., Duckworthdagger, D., and Randall, A. (2001). *J. Physiol.* **533**, 467–478.
Guia, A., Stern, M. D., Lakatta, E. G., and Josephson, I. R. (2001). *Biophys. J.* **80**, 2742–2750.
Heginbotham, L., Abramson, T., and MacKinnon, R. (1992). *Science* **258**, 1152–1155.
Heidelberger, R., and Matthews, G. (1992). *J. Physiol.* **447**, 235–256.
Heinemann, S. H., Terlau, H., Stühmer, W., Imoto, K., and Numa, S. (1992). *Nature* **356**, 441–443.
Hering, S., Berjukow, S., Aczel, S., and Timin, E. N. (1998). *Trends Pharmacol. Sci.* **19**, 439–443.
Hering, S., Berjukow, S., Sokolov, S., Marksteiner, R., Weiss, R. G., Kraus, R., and Timin, E. N. (2000). *J. Physiol.* **528**, 237–249.
Herlitze, S., Garcia, D. E., Mackie, K., Hille, B., Scheuer, T., and Catterall, W. A. (1996). *Nature* **380**, 258–262.
Herlitze, S., Xie, M., Han, J., Hümmer, A., and Mark, M. D. (2003). *J. Bioenerg. Biomembr.* **35**, 621–638.
Hille, B. (2001). *Ion Channels of Excitable Membranes*, 3rd edn. Sinauer, Sunderland, MA.
Hodgkin, A. L., and Huxley, A. F. (1952a). *J. Physiol.* **116**, 473–496.
Hodgkin, A. L., and Huxley, A. F. (1952b). *J. Physiol.* **116**, 449–472.
Hodgkin, A. L., and Huxley, A. F. (1952c). *J. Physiol.* **117**, 500–544.
Hoshi, T., Zagotta, W. N., and Aldrich, R. W. (1990). *Science* **250**, 533–538.
Ikeda, S. R. (1996). *Nature* **380**, 255–258.
Jarvis, S. E., and Zamponi, G. W. (2001). *Trends Pharmacol. Sci.* **22**, 519–525.
Jiang, Y., Lee, A., Chen, J., Cadene, M., Chait, B. T., and MacKinnon, R. (2002). *Nature* **417**, 523–526.
Jiang, Y., Lee, A., Chen, J., Ruta, V., Cadene, M., Chait, B. T., and MacKinnon, R. (2003a). *Nature* **423**, 33–41.
Jiang, Y., Ruta, V., Chen, J., Lee, A., and MacKinnon, R. (2003b). *Nature* **423**, 42–48.
Jones, S. W. (1987). *J. Physiol.* **389**, 605–627.
Jones, S. W. (1998). *J. Bioenerg. Biomembr.* **30**, 299–312.
Jones, S. W. (2002). *J. Physiol.* **545**, 334.
Jones, S. W., and Marks, T. N. (1989a). *J. Gen. Physiol.* **94**, 151–167.
Jones, S. W., and Marks, T. N. (1989b). *J. Gen. Physiol.* **94**, 169–182.
Katz, B., and Miledi, R. (1967). *J. Physiol.* **189**, 535–544.
Klemic, K. G., Durand, D. M., and Jones, S. W. (1998). *J. Neurophysiol.* **79**, 2345–2357.
Klemic, K. G., Kirsch, G. E., and Jones, S. W. (2001). *Biophys. J.* **81**, 814–826.
Klugbauer, N., Dai, S. P., Specht, V., Lacinova, L., Marais, E., Bohn, G., and Hofmann, F. (2000). *FEBS Lett.* **470**, 189–197.
Klugbauer, N., Marais, E., and Hofmann, F. (2003). *J. Bioenerg. Biomembr.* **35**, 639–648.
Koschak, A., Reimer, D., Huber, I. G., Grabner, M., Glossmann, H., Engel, J., and Striessnig, J. (2001). *J. Biol. Chem.* **276**, 22100–22106.
Kuo, C.-C., and Bean, B. P. (1994). *Neuron* **12**, 819–829.
Lacinova, L., Klugbauer, N., and Hofmann, F. (1999). *J. Physiol.* **516**, 639–645.
Lacinova, L., Klugbauer, N., and Hofmann, F. (2002). *FEBS Lett.* **531**, 235–240.
Lipkind, G. M., and Fozzard, H. A. (2000). *Biochemistry* **39**, 8161–8170.
Lipkind, G. M., and Fozzard, H. A. (2001). *Biochemistry* **40**, 6786–6794.
Liu, Y., Jurman, M. E., and Yellen, G. (1996). *Neuron* **16**, 859–867.
Llinas, R., Steinberg, I. Z., and Walton, K. (1981a). *Biophys. J.* **33**, 289–321.
Llinas, R., Steinberg, I. Z., and Walton, K. (1981b). *Biophys. J.* **33**, 323–351.
MacKinnon, R. (1995). *Neuron* **14**, 889–892.
Marchetti, C., Amico, C., and Usai, C. (1995). *J. Neurophysiol.* **73**, 1169–1180.
Marks, T. N., and Jones, S. W. (1992). *J. Gen. Physiol.* **99**, 367–390.
McCleskey, E. W., and Almers, W. (1985). *Proc. Natl. Acad. Sci. U.S.A.* **82**, 7149–7153.
McCobb, D. P., and Beam, K. G. (1991). *Neuron* **7**, 119–127.
Meinrenken, C. J., Borst, J. G., and Sakmann, B. (2003). *J. Physiol.* **547**, 665–689.
Monod, J., Wyman, J., and Changeux, J.-P. (1965). *J. Mol. Biol.* **12**, 88–118.
Montell, C., Birnbaumer, L., and Flockerzi, V. (2002). *Cell* **108**, 595–598.
Nakai, J., Sekiguchi, N., Rando, T. A., Allen, P. D., and Beam, K. G. (1998). *J. Biol. Chem.* **273**, 13403–13406.
Nonner, W., and Eisenberg, B. (1998). *Biophys. J.* **75**, 1287–1305.
Obejero-Paz, C. A., Jones, S. W., and Scarpa, A. (1991). *J. Gen. Physiol.* **98**, 1127–1140.
Ohana, O., and Sakmann, B. (1998). *J. Physiol.* **513**, 135–148.
Pan, Z. H., Hu, H. J., Perring, P., and Andrade, R. (2001). *Neuron* **32**, 89–98.
Patil, P. G., Brody, D. L., and Yue, D. T. (1998). *Neuron* **20**, 1027–1038.
Patlak, J. (1991). *Physiol. Rev.* **71**, 1047–1080.
Perez-Reyes, E. (2003). *Physiol. Rev.* **83**, 117–161.
Peterson, B. Z., DeMaria, C. D., Adelman, J. P., and Yue, D. T. (1999). *Neuron* **22**, 549–558.
Plummer, M. R., and Hess, P. (1991). *Nature* **351**, 657–659.
Poage, R. E., and Meriney, S. D. (2002). *Physiol. Behav.* **77**, 507–512.
Protasi, F., Paolini, C., Nakai, J., Beam, K. G., Franzini-Armstrong, C., and Allen, P. D. (2002). *Biophys. J.* **83**, 3230–3244.
Qiao, X., and Meng, H. (2003). *J. Bioenerg. Biomembr.* **35**, 661–670.
Ríos, E., and Stern, M. D. (1997). *Annu. Rev. Biophys. Biomol. Struct.* **26**, 47–82.
Roberts, W. M., Jacobs, R. A., and Hudspeth, A. J. (1990). *J. Neurosci.* **10**, 3664–3684.
Rubart, M., Patlak, J. B., and Nelson, M. T. (1996). *J. Gen. Physiol.* **107**, 459–472.
Rudy, B. (1978). *J. Physiol.* **283**, 1–21.
Ruta, V., Jiang, Y., Lee, A., Chen, J., and MacKinnon, R. (2003). *Nature* **422**, 180–185.
Sabatini, B. L., and Regehr, W. G. (1996). *Nature* **384**, 170–172.
Sabatini, B. L., and Regehr, W. G. (1999). *Annu. Rev. Physiol.* **61**, 521–542.
Sanchez, J. A., and Stefani, E. (1983). *J. Physiol.* **337**, 1–17.
Schoppa, N. E., and Sigworth, F. J. (1998). *J. Gen. Physiol.* **111**, 313–342.
Schouten, V. J., and Morad, M. (1989). *Pflügers Arch.* **415**, 1–11.
Scroggs, R. S., and Fox, A. P. (1992). *J. Neurosci.* **12**, 1789–1801.
Serrano, J. R., Perez-Reyes, E., and Jones, S. W. (1999). *J. Gen. Physiol.* **114**, 185–201.
Sheng, Z.-H., Rettig, J., Takahashi, M., and Catterall, W. A. (1994). *Neuron* **13**, 1303–1313.

Soldatov, N. M. (2003). *Trends Pharmacol. Sci.* **24**, 167–171.
Soler-Llavina, G. J., Holmgren, M., and Swartz, K. J. (2003). *Neuron* **38**, 61–67.
Staes, M., Talavera, K., Klugbauer, N., Prenen, J., Lacinova, L., Droogmans, G., Hofmann, F., and Nilius, B. (2001). *J. Physiol.* **530**, 35–45.
Stanley, E. F. (1997). *Trends Neurosci.* **20**, 404–409.
Stotz, S. C., and Zamponi, G. W. (2001). *Trends Neurosci.* **24**, 176–182.
Stühmer, W., Conti, F., Suzuki, H., Wang, X. D., Noda, M., Yahagi, N., Kubo, H., and Numa, S. (1989). *Nature* **339**, 597–603.
Swandulla, D., and Armstrong, C. M. (1989). *Proc. Natl. Acad. Sci. U.S.A.* **86**, 1736–1740.
Tareilus, E., Roux, M., Qin, N., Olcese, R., Zhou, J., Stefani, E., and Birnbaumer, L. (1997). *Proc. Natl. Acad. Sci. U.S.A.* **94**, 1703–1708.
Thévenod, F., and Jones, S. W. (1992). *Biophys. J.* **63**, 162–168.
Voets, T., and Nilius, B. (2003). *J. Membr. Biol.* **192**, 1–8.
Werz, M. A., Elmslie, K. S., and Jones, S. W. (1993). *Pflügers Arch.* **424**, 538–545.
West, J. W., Patton, D. E., Scheuer, T., Wang, Y., Goldin, A. L., and Catterall, W. A. (1992). *Proc. Natl. Acad. Sci. U.S.A.* **89**, 10910–10914.
Wu, L. G., Borst, J. G. G., and Sakmann, B. (1998). *Proc. Natl. Acad. Sci. U.S.A.* **95**, 4720–4725.
Wu, L. G., Westenbroek, R. E., Borst, J. G. G., Catterall, W. A., and Sakmann, B. (1999). *J. Neurosci.* **19**, 726–736.
Xu, W., and Lipscombe, D. (2001). *J. Neurosci.* **21**, 5944–5951.
Yang, J., Ellinor, P. T., Sather, W. A., Zhang, J. F., and Tsien, R. W. (1993). *Nature* **366**, 158–161.
Yazejian, B., Sun, X. P., and Grinnell, A. D. (2000). *Nat. Neurosci.* **3**, 566–571.
Yunker, A. M. R., and McEnery, M. W. (2003). *J. Bioenerg. Biomembr.* **35**, 533–576.
Zagotta, W. N., and Aldrich, R. W. (1990). *J. Gen. Physiol.* **95**, 29–60.
Zagotta, W. N., Hoshi, T., and Aldrich, R. W. (1994). *J. Gen. Physiol.* **103**, 321–362.
Zhang, J.-F., Ellinor, P. T., Aldrich, R. W., and Tsien, R. W. (1994). *Nature* **372**, 97–100.
Zheng, J., and Sigworth, F. J. (1998). *J. Gen. Physiol.* **112**, 457–474.
Zhong, H. J., Yokoyama, C. T., Scheuer, T., and Catterall, W. A. (1999). *Nat. Neurosci.* **2**, 939–941.
Zühlke, R. D., Pitt, G. S., Deisseroth, K., Tsien, R. W., and Reuter, H. (1999). *Nature* **399**, 159–162.